Published in final edited form as:

Clin Cancer Res. 2023 April 03; 29(7): 1292–1304. doi:10.1158/1078-0432.CCR-22-3379.

IL-6 mediates suppression of T and NK cells function in EMT-associated TKI-resistant EGFR mutant NSCLC

Sonia A. Patel[1], **Monique B. Nilsson**[1], **Yan Yang**[1], **Xiuning Le**[1], **Hai Tran**[1], **Yasir Y. Elamin**[1], **Xiaoxing Yu**[1], **Fahao Zhang**[1], **Alissa Poteete**[1], **Xiaoyang Ren**[1], **Li Shen**[2], **Jing Wang**[2], **Seyed Javad Moghaddam**[3], **Tina Cascone**[1], **Michael Curran**[4], **Don L. Gibbons**[1], **John V. Heymach**[1]

[1]Department of Thoracic/Head and Neck Medical Oncology, The University of Texas M. D. Anderson Cancer Center, Houston, Texas 77130.

[2]Department of Bioinformatics and Computational Biology, The University of Texas M. D. Anderson Cancer Center, Houston, Texas 77130.

[3]Department of Pulmonary Medicine, The University of Texas M. D. Anderson Cancer Center, Houston, Texas 77130.

[4]Department of Immunology, The University of Texas M. D. Anderson Cancer Center, Houston, Texas 77130.

Abstract

Purpose: Advanced non-small cell lung cancer (NSCLC) patients harboring activating epidermal growth factor receptor (EGFR) mutations are initially responsive to tyrosine kinase inhibitors (TKIs). However, therapeutic resistance eventually emerges, often via secondary EGFR mutations or EGFR-independent mechanisms such as EMT. Treatment options after EGFR-TKI resistance are limited as anti-PD-1/PD-L1 inhibitors typically display minimal benefit. Given that IL-6 is associated with worse outcomes in NSCLC patients, we investigate if IL-6 in part contributes to this immunosuppressed phenotype.

Experimental Design: We utilized a syngeneic genetically engineered mouse model (GEMM) of EGFR mutant NSCLC to investigate the effects of IL-6 on the tumor microenvironment and the combined efficacy of IL-6 inhibition and anti-PD1 therapy. Corresponding in vitro studies used EGFR mutant human cell lines and clinical specimens.

Results: We identified that EGFR mutant tumors which have oncogene-independent acquired resistance to EGFR-TKIs were more mesenchymal and had markedly enhanced IL-6 secretion. In EGFR mutant GEMMs, IL-6 depletion enhanced activation of infiltrating NK and T cell subpopulations and decreased immunosuppressive T-regulatory and Th17 cell populations. Inhibition of IL-6 increased NK and T cell -mediated killing of human osimertinib-resistant EGFR mutant NSCLC tumor cells in cell culture. IL-6 blockade sensitized EGFR mutant GEMM tumors to PD-1 inhibitors through an increase in tumor-infiltrating IFNγ+ CD8+ T cells.

Corresponding Author: John V. Heymach, MD, PhD, Departments of Thoracic and Head and Neck Medical Oncology and Cancer Biology, Unit 432, The University of Texas MD Anderson Cancer Center, 1515 Holcombe Blvd, Houston, TX 77030, USA; phone: 713-792-6363; fax: 713-792-1220; jheymach@mdanderson.org.

The remaining authors declare no conflicts of interest.

Conclusions: These data indicate that IL-6 is upregulated in EGFR mutant NSCLC tumors with acquired EGFR-TKI resistance and suppressed T and NK cell function. IL-6 blockade enhanced antitumor immunity and efficacy of anti-PD1 therapy warranting future clinical combinatorial investigations.

Keywords

Non-small cell lung cancer; epidermal growth factor receptor; tumor microenvironment; interleukin-6; immunosuppression

Introduction

Non-small cell lung cancer (NSCLC) is the leading cause of cancer deaths worldwide. Around 10–15% of NSCLC patients in the United States and up to 40% in the Asian population bear tumors harboring activating mutations in the epidermal growth factor receptor (EGFR) [1]. For patients with advanced disease, EGFR tyrosine kinase inhibitors (TKIs) such as the third-generation drug osimertinib are part of standard first-line therapy. While the vast majority of patients initially benefit from EGFR-TKIs, therapeutic resistance can emerge via either EGFR-dependent mechanisms, such as secondary EGFR mutations (e.g. C797S mutations), or via EGFR-independent mechanisms such as or epithelial-to-mesenchymal transition (EMT) or small cell transformation [2–4]. For patients with TKI resistance, standard treatment approaches are limited and include chemotherapy and immunotherapy with anti-PD-1/PD-L1 immune checkpoint-blockade (ICB). Because immunotherapy is typically employed after the use of EGFR-TKI, there is a major unmet need for new treatment approaches for these patients.

Patients with EGFR mutant NSCLC are typically resistant to ICB. In the TKI naïve setting, an objective response rate of 9% was observed for the PD-1 inhibitor pembrolizumab, and enrollment to this phase II trial (NCT02879994) was ceased early due to lack of efficacy [5]. In the TKI-resistant setting, response rates were even lower, with objective response rates to ICB typically less than 5% [6–12]. The mechanisms driving immunotherapy resistance in EGFR mutant NSCLC are not well understood and are likely multi-factorial. In comparison to EGFR-wildtype tumors, EGFR mutant tumors have been reported to have a lower tumor mutational burden and expression of PD-L1, factors implicated in ICB resistance [13]. However EGFR mutant NSCLC patients appear to still have significantly lower response rates [12] than patients bearing EGFR-wildtype tumors, even in tumors expressing high levels of PD-L1.

Tumor-derived immunomodulators such as cytokines are known to impact the tumor immune microenvironment and immunotherapy response. We and others reported that IL-6 is a potential mediator of resistance to first-generation TKIs [14, 15] that occurs independent of secondary EGFR mutations or *MET* amplification. Given the known immunomodulatory role of IL-6, in the present report we sought to investigate whether IL-6 promotes an immunologically inert phenotype in EGFR mutant TKI-refractory tumors and whether blockade of IL-6 might enhance the activity of ICB therapy in EGFR mutant NSCLC tumors.

Here we report that IL-6 inhibited the activation of T and NK cells in the EGFR mutant tumor microenvironment. In genetically engineered mouse models (GEMMs) of EGFR mutant NSCLC, knockout of IL-6 extended overall survival and enhanced immune cell infiltration. Moreover, IL-6 null tumors had reduced T-regulatory and Th17 T cell populations, which are implicated as contributing to tumor immunosuppression. Additionally, depletion of IL-6 resulted in increased infiltration of activated NK cells in vivo, and acute blockade of IL-6 further sensitized EGFR mutant cell lines to NK-mediated cytotoxic killing. Blockade of IL-6 in combination with anti-PD-1 treatment increased tumor infiltration by activated CD8 T cells and extended overall survival of tumor-bearing animals. Our findings indicate that blockade of IL-6 signaling reduces tumor immunosuppression and enhances both anti-tumor immunity and responsiveness to anti-PD-1 immunotherapy within the ICB-resistant, EGFR mutant subset of NSCLC.

Materials and Methods

Cell culture and reagents:

NSCLC cell lines HCC4006, HCC827, and H1975 were obtained from ATCC and maintained as previously described [16]. EGFR-TKI resistant cell lines were generated as previously described [3]. YUL-0019 (N771delinsFH) [17] were obtained by Dr. Politi (Yale Medical School). MDA-L-011 (L858R) [3], MDA-L-004K (EGFR exon 20 mutation), MDA-L-0024 (E746_A750del mutation), MDA-L-0046 (EGFR exon 19 del), and MDA-L-0065 (EGFR exon 19 del) were derived from patients at MD Anderson that progressed on EGFR-TKIs and were cell lines generated from surgical specimens collected after patients provided written informed consent through an Institutional Review Board-approval protocol at MD Anderson Cancer and conducted in accordance with the Declaration of Helsinki and Belmont report. All cell lines were cultured in RPMI medium supplemented with 10% FBS, 1% penicillin-streptomycin, and 1% L-glutamine. IL-6 neutralizing antibodies were obtained from R&D Systems. Erlotinib and siltuximab were obtained from the institutional pharmacy at the University of Texas MD Anderson Cancer Center.

Flow Cytometry:

The following mouse flow cytometry conjugated antibodies were used at the concentration suggested on the manufacturer's data sheet for surface or intracellular staining: Live/Dead Ghost UV450, anti-CD45 BUV805, anti-PD1 BV421, anti-CD8 BV570, anti-NKG2D FITC, anti-CD278 BV785, anti-IFNγ PerCP-Cy5.5, anti-PD-L1 PE-Dazzle 594, anti-NK1.1 Pe-CY5, anti-CD3 Pe-Fire700, anti-CD4 AlexaFluor700, anti-Ki-67 Pacific Blue, anti-FoxP3 Alexa532, anti-Granzyme B PE, anti-IL-17A APC all purchased from Biolegend or Thermofisher. For intracellular staining of FoxP3, Granzyme B, IL-17A, and Ki-67, the cells were fixed and permeabilized using cold 70% ethanol. Immuno-stained cell percentages were assessed by a Cytek Aurora flow cytometer and analyzed by Flow-Jo software.

Multiplex cytokine array:

Mouse Luminex discovery assay was performed on mouse serum collected from blood of $EGFR^{L858R}$ GEMMs.

Detection of IL-6 in preclinical samples:

NSCLC cells (200,000 cells/well in 6-well plates) were plated in 10% FBS serum RPMI medium and after 24 hours were replaced with serum-free medium, and then conditioned medium was collected. IL-6 ELISA (R&D Systems) was performed according to manufacturer's instructions. For IL-6 staining, antibodies (1:50; Millipore) were used on formalin-fixed paraffin-embedded tumor sections. For inhibitor studies, cells were pre-treated with human IL-6 inhibitor as described [14].

Detection of IL-6 in clinical samples:

Biospecimens were obtained after patients provided written informed consent under an Institutional Review Board approved protocol and conducted in accordance with the Declaration of Helsinki and Belmont report. The CROSSOVER and NORTHSTAR datasets include patients from MD Anderson who received osimertinib treatment and if applicable local consolidated therapy. We analyzed 12 matched pairs of samples collected prior to progression of disease (after randomization and end of cycle2 of osimertinib treatment) and at progression of disease. Each sample was analyzed in duplicate and analysis of circulating IL-6 concentration was performed. Groups were compared using a paired two-tailed Student's t-test.

RT-PCR:

Total cellular RNA was isolated using TRIzol Reagent (Invitrogen) and RT-PCR was performed in triplicate biological samples.

Reverse phase protein array:

Whole cell lysates were collected as previously described [18] with protein expression quantified by using the SuperCurve method [19]. Statistics analyses of RPPA data were performed by using R packages [20].

RNA-sequencing:

Total RNA was collected from the EGFR mutant NSCLC GEMM models listed above and extracted and purified using the RNeasy Plus Mini Kit (Qiagen). RNA-seq libraries were prepared and analyzed in triplicate using the Illumina Mouse NovaSeq6000. Human EGFR mutant NSCLC cell line gene expression data from the GEO repository (GSE 121634) has also been utilized [3].

Functional immune cell assays:

Human peripheral blood mononuclear cells (PBMC) from healthy donors purchased from the Gulf coast consortium were obtained from whole blood samples and isolated by Ficoll-Paque density gradient centrifugation. The ex vivo expansion and activation of NK cells used K562 feeder cells (1:2 ratio) and 200 U/mL IL-2 and 5 ng/mL IL-15, and 2 mM GlutaMAX purchased from Gibco. Healthy donor-derived NK cells were cultured in RPMI medium supplemented with 10% FBS, 1% penicillin-streptomycin, and 1% L-glutamine. Cells were cultured for 14 days and counted using trypan blue. To isolate T cells, PBMCs were activated with anti-CD3/CD28 Dynabeads (Thermo Fischer Scientific) at a 1:1 ratio

in RPMI-1640 complete media (10% FBS, 2 mM GlutaMAX, 100 U/mL penicillin, and 100 μg/mL streptomycin) supplemented with 100 U/mL IL-2 (PreproTech). To assess cytotoxicity in vitro, NK or T cells were co-cultured with target cells stably transfected with pHIV-Luc-ZsGreen (Addgene plasmid # 39196) and plated at varying effector to target ratios (10:1, 5:1, 2.5:1, and 1:1). Cytotoxic killing was quantified by luciferase signal after 4 hours of incubation. This signal was quantified using a FLUOstar OPTIMA multi-mode micro-plate reader (BMG Labtech). Specific lysis was calculated using ((Target cells only–Experimental Target) / (Target cells only – no target cells) × 100). Similar assays were performed with T cells derived from healthy donors. Target cells for T cell cytotoxicity assay were transduced with luciferase pHIV-Luc-ZsGreen (Addgene plasmid #39196) and custom OKT3 construct (pPSFG-OKT3-CD86).

In vivo studies:

CCSP-rtTA EGFR^{L858R} genetically engineered mice were obtained from Dr. Katherine Politi (Yale School of Medicine) [21]. Mice were crossed with IL-6 knockout mice (IL6$^{-/-}$) obtained from Dr. Seyed Moghaddam (MD Anderson Cancer Center) to generate CCSP-rtTA EGFR^{L858R}/IL-6$^{-/-}$ mice. After 6 weeks of doxycycline diet treatment, animals were randomized into treatment groups and treated with a monoclonal antibody against IL-6 (10 mg/kg) or anti-PD-1 (10 mg/kg), intra-peritoneally, twice a week. Antibodies were purchased from Bioxcell. Tumors and serum from mice were harvested after three weeks.

Immunohistochemistry:

Frozen tissue sections were used to evaluate EMT and immune cell markers. Specimens were sectioned (8–10 μM thickness) and stained with antibodies against E-cadherin, vimentin, SP-C, and TTF-1 at 4°C overnight. Staining was visualized using an AxioCam MRC5 camera and Axio vision software 4.6.

Timer2.0 analysis:

This immune deconvolution tool used RNA-sequencing data analysis to estimate immune infiltrates through comparison of multiple deconvolution analyses [22].

KMplotter analysis:

1926 NSCLC patients from the KMplotter lung cancer database were stratified across expression level of IL-6 and evaluated for overall survival in months.

Statistics:

For all studies, statistical analysis was performed using the Student's *t*-test (two-tailed) or one-way ANOVA. A p value ≤ 0.05 was considered statistically significant (*), p ≤ 0.01 (**), and p ≤ 0.001 (***). For RNA-sequencing data, analysis of variance (ANOVA) was used on a gene by gene basis. The resulting *P* values, computed from F-statistic, were modeled using the beta-uniform mixture (BUM) model and used to determine a false discovery rate (FDR) cutoff to identify significantly differentially expressed genes.

Data availability:

Gene expression data from human EGFR mutant NSCLC cell lines have been uploaded to the GEO repository (GSE 121634) as previously reported [3]. Additional raw data for this study were generated at MD Anderson Cancer Center, and data related to this study are available from the corresponding author upon request.

Results

IL-6 secretion is elevated in human EGFR mutant NSCLC cells with acquired TKI resistance

We and others have shown that EGFR mutant NSCLC cells with acquired resistance to the first-generation EGFR inhibitor, erlotinib, overexpress IL-6 [14, 15]. To determine whether IL-6 is similarly elevated in human NSCLC cell lines with acquired resistance to the third-generation EGFR-TKI osimertinib, we utilized a panel of osimertinib refractory cell lines previously shown to have undergone EGFR-TKI resistance [3] through epithelial to mesenchymal transition (EMT) [3]. In our models of EGFR TKI resistance mediated by MET amplification, IL-6 was not upregulated [14]. Osimertinib-resistant (OR) variants secreted significantly greater levels of IL-6 compared to EGFR mutant parental cells HCC4006 (Fig 1A) ($p = 0.0063$) and H1975 (Fig 1B) ($p = 0.0040$). Likewise, *IL-6* RNA levels were upregulated in EGFR-TKI resistant cells as compared to parental (Supplemental Fig 1A). We tested IL-6 secretion by YUL-0019 cells which harbor an exon 20 insertion (N771del insFH) and are sensitive to poziotinib along with their poziotinib-resistant variants that we previously reported had undergone EMT [23]. YUL-0019 parental cells expressed low levels of IL-6, whereas, poziotinib-resistant cells expressed significantly higher levels of IL-6 (Supplemental Fig 1B).

Next, we sought to determine whether IL-6 production was also upregulated in patient-derived models of EGFR-TKI resistance. Therefore, we generated cell lines from EGFR mutant patients who progressed on EGFR-TKIs and evaluated IL-6 secretion by ELISA. Patient-derived models of acquired EGFR-TKI resistance (MDA-L-004K, MDA-L0011, MDA-L-0024, MDA-L-0046, and MDA-L-0065) secreted higher amounts of IL-6 as compared to EGFR mutant TKI-naïve cells (Fig 1C). We also observed increases in *IL6* mRNA expression in tumors from EGFR mutant, TKI refractory patients as compared to TKI-naïve EGFR mutant tumors from the MD Anderson GEMINI dataset (Supplemental Fig 1C) ($p = 0.050$), and these TKI refractory specimens also displayed a mesenchymal phenotype as indicated by increased expression of *ZEB1* and decreased expression of *CDH1* (Supplemental Fig 1D&E). To investigate whether high IL-6 was associated with a worse clinical outcome in NSCLC patients, we utilized the lung cancer KMplotter and found that high expression of *IL6* was associated with a worse overall survival ($HR = 1.48$, $p < 0.0001$) than those with low expression of *IL6* (Fig 1D). Moreover, after investigating serum of patients enrolled in the MD Anderson CROSSOVER and NORTHSTAR clinical trial studies, we identified that circulating IL-6 levels were higher in patients with progressive disease compared to blood from these same patients collected prior to progression of disease (Fig 1E) ($p=0.0517$).

Depletion of IL-6 increases overall survival and number of activated infiltrating lymphocytes in murine immunocompetent EGFR mutant NSCLC tumor models

To evaluate the impact of IL-6 on EGFR mutant NSCLC tumor growth and the tumor immune microenvironment (TIME), we utilized syngeneic, immune competent murine models. To do this, we crossed the doxycycline-inducible $EGFR^{L858R}$ GEMM model [21] with IL-6 KO mice (Supplemental Fig 2A–B). As expected, concentrations of IL-6 were essentially eliminated in the serum and bronchoalveolar lavage fluid (BALF) in $EGFR^{L858R}/IL6^{tKO}$ mice as compared to $EGFR^{L858R}$ mice (Figure 2A). Immunohistochemistry staining validated the absence of IL-6 protein in tumors from $EGFR^{L858R}/IL6^{tKO}$ mice (Supplemental Fig 2C). Depletion of IL-6 in treatment naïve EGFR ^{L858R} mice had a modest yet significant effect on survival (Fig 2B; HR = 1.31, p=0.0212). Interestingly, treatment naïve $EGFR^{L858R}/IL6^{tKO}$ tumors displayed increased necrotic area which may be indicative of increased cell death in the absence of IL-6 (Supplemental Fig 2D).To investigate the effects of IL-6 on the tumor immune microenvironment of EGFR mutant tumors, we next analyzed $EGFR^{L858R}$ and $EGFR^{L858R}/IL6^{tKO}$ tumors by RNA-sequencing data and performed immune cell deconvolution analysis. IL-6 depletion resulted in increased NK cell populations within the tumor (Fig 2C; p=0.0032). Moreover, knockout of IL6 increased the CD8+ T cell ($p<0.0001$) and T follicular helper cell populations ($p<0.0001$) while populations of T-regulatory cells (p=0.1004) decreased within the tumor (Fig 2D). Flow cytometry analysis was performed to further analyze the presence of tumor-infiltrating immune cells in EGFR mutant tumors with or without IL-6. Total immune infiltration in tumors from $EGFR^{L858R}/IL6^{tKO}$ trended toward a higher density compared to $EGFR^{L858R}$ (p=0.06) (Fig 2E). Moreover, NK cell (p=0.0471) and T cell (p=0.0408) infiltration was significantly increased in $EGFR^{L858R}/IL6^{tKO}$ tumors as compared to $EGFR^{L858R}$ tumors (Fig 2E). Among T cell subtypes, the CD4+ T cell population was more notably increased with IL-6 depletion (p=0.0086) as compared to CD8+ T cells (p=0.0595), and the Foxp3+ T-regulatory population was not significantly altered.

Given our finding that tumor immune infiltration was enhanced in EGFR mutant tumors with IL-6 knockout, we next assessed whether blockade of IL-6 signaling could similarly alter the tumor immune microenvironment. Tumors were initiated in $EGFR^{L858R}$ mice, and animals were randomized to receive control antibodies or anti-IL-6 blocking antibodies. IL-6 blockade significantly extended the overall survival of tumor-bearing animals (HR = 2.301, p=0.0385; Fig 2F). Moreover, consistent with the knockout experiment, we observed an increase in infiltration of NK and CD4+ T cells in the tumor microenvironment as determined by flow cytometry (Fig 2G) in mice treated with IL-6 blockade. Collectively, these data indicated that IL-6 in TKI naïve EGFR mutant NSCLC tumors causes a reduction in NK and T lymphocytic infiltration, particularly in CD4+ T cells, which can be restored with IL-6 blockade.

EGFR mutant NSCLC tumors with acquired EGFR-TKI resistance associated with EMT display an immunologically cold phenotype and secrete IL-6

As there are currently no established syngeneic murine models of EGFR-independent TKI resistance to facilitate the study of the tumor immune microenvironment, we used an approach previously described for KRAS [24, 25] and other oncogenes of “extinguishing”

the driver oncogene using an inducible system after tumors were established. We chose to investigate TKI resistance in this setting because due to the reduced tumor burden in syngeneic EGFR mutant models, it is not likely that osimertinib resistance emerges with continuous dosing at therapeutic levels, although some investigators have used dosing of osimertinib for a limited period of time (e.g. 2 weeks) followed by drug discontinuation to evaluate post-tumor regrowth [26]. To establish this driver extinguishing model, we used the doxycycline-inducible $EGFR^{L858R}$ GEMM model [21] with chow containing doxycycline (DOX) to induce tumor growth (oncogene-dependent tumors; Fig 3A). To develop oncogene-independent resistance in the $EGFR^{L858R}$ GEMM model, we likewise induced expression using doxycycline-containing chow, and then after 6 weeks when lung tumors could be visualized by CT imaging, doxycycline chow was withdrawn in an effort to mimic the development of EGFR-TKI resistance that occurs independently of EGFR secondary mutations (oncogene-independent tumors; Fig. 3A). The withdrawal of doxycycline was initially associated with loss of mutant EGFR expression (Fig 3B) and initial tumor shrinkage followed by resumed tumor growth (Supplemental Fig 3A). To confirm that oncogene-independent tumors were EGFR-TKI resistant, animals were treated with or without osimertinib for 2 weeks. As observed by CT imaging (Fig 3C), osimertinib treatment led to a marked reduction in the volume of oncogene-dependent tumors ($p=0.0002$), while oncogene-independent tumors increased in size ($p = 0.0475$; Fig 3D).

Next, we evaluated the molecular changes associated with acquired EGFR independence. After verification of the tumor by pathology (Supplemental Fig 3B–C), tumor tissue from oncogene-independent and oncogene-dependent tumors was evaluated by RNA-seq and gene set enrichment analysis (GSEA) which revealed an enrichment in EMT-associated gene expression (Fig 3E). The shift towards a mesenchymal phenotype in the oncogene-independent tumors was confirmed by immunohistochemistry showing increased expression of vimentin and decreased expression of E-cadherin in oncogene-independent tumors compared to oncogene-dependent tumors (Fig 3F). Previous studies have shown an association between a mesenchymal phenotype and a cold immune microenvironment in lung adenocarcinomas [27]. Therefore, we hypothesized that oncogene-independent (mesenchymal) tumors may display a colder immune microenvironment compared to the oncogene-dependent (epithelial) tumors. Immune cell deconvolution analysis revealed significantly decreased CD8+ T cells ($p=0.0194$), CD4+ T cells ($p <0.0001$), T regulatory cells ($p = 0.0061$) total NK cells ($p <0.0001$), and decreased activated NK cells ($p=0.0122$) in oncogene-independent tumors as compared to oncogene-dependent tumors (Fig 3G&H).

We next evaluated expression of 16 immunomodulatory-related cytokines in the serum from mice bearing oncogene-dependent and oncogene-independent tumors by multiplex ELISA and found that IL-6 and IL-9 were the most highly upregulated cytokines in oncogene-independent tumor bearing animals as compared to oncogene-dependent tumor-bearing animals (Fig 3I). Increased circulating levels of IL-6 and tumor levels of IL-6 in oncogene-independent mice was confirmed by ELISA assay and immunohistochemistry (IHC), respectively (Fig 3J, Supplemental Fig 3D). Collectively, these data show that IL-6 is upregulated in EGFR mutant NSCLC tumors which have developed oncogene-independent, EMT-associated TKI resistance.

IL-6 suppresses NK cell activation in EGFR mutant NSCLC tumors

IL-6 signaling has been shown to impair NK activity in other cancer types [28]. Thus, we next assessed whether IL-6 modulates NK cell proliferation in EGFR mutant tumors. As determined by IHC, NK cell proliferation was similar in $EGFR^{L858R}$ tumors with or without IL-6 knockout (Fig 4A). Likewise, treatment of $EGFR^{L858R}$ tumor-bearing mice with anti-IL-6 antibodies did not affect NK cell proliferation (Fig 4B; Supplemental Fig 4A). However, the number of activated NKG2D+ NK cells was increased by IL-6 depletion or antibody-mediated IL-6 blockade (Fig 4C&D, Supplemental Fig 4B). To further investigate the impact of IL-6 on NK activation markers, NK cells isolated from healthy donor peripheral blood mononuclear cells (PBMCs) were expanded *ex vivo* (Supplemental Fig 4C) and then incubated in conditioned media collected from human HCC4006 EGFR mutant cell lines and their osimertinib-resistant (OR) variants alone or in combination with the IL-6 antibody siltuximab. After 48 hours, NK cells were analyzed by flow cytometry. IL-6 blockade enhanced expression of the NK activation marker NKG2D in NK cells cultured in conditioned media from HCC4006 OR cells (Fig 4E), but not parental HCC4006 cells. Similarly, IL6 blocking antibodies increased granzyme B expression in NK cells incubated in HCC4006 OR4 and OR7 (Fig 4F). However, perforin expression, which is an indicator of cytotoxic potential, was not altered in NK cells treated with OR cell conditioned media or anti-IL6 (Supplemental Fig 4D). NK activation and inhibitory receptors can bind to corresponding ligands expressed on tumor cells. Thus, we investigated the effect of IL-6 on tumor cell expression of NK receptor ligands. Treatment of HCC4006 OR cells with IL-6 neutralizing antibodies increased expression of MICA, a NK activation ligand which typically binds to NKG2D+ NK cells (Fig 4G), and enhanced expression of ULBP1, another NK activation ligand (Supplemental Fig 4E), although expression of HLA-E, a NK inhibitory ligand which typically binds inhibitory NK cells, was not significantly different between parental and osimertinib resistant cells with or without IL-6 antibodies (Supplemental Fig 4F).

We next assessed whether human EGFR-TKI resistant cells that have acquired EGFR-TKI resistance through EMT-mediated mechanisms are sensitive to NK-mediated killing and whether inhibition of IL-6 can enhance this effect. We hypothesized that IL-6 blockade would enhance NK-mediated killing of TKI-resistant EGFR mutant cells to a greater extent than TKI-naïve cells. Consistent with this hypothesis, we observed that while IL-6 neutralizing antibodies did not impact NK-mediated killing of HCC4006 parental cells (low IL-6 expressing), blockade of IL-6 did sensitize EGFR mutant TKI-refractory cell lines to NK-mediated cytotoxic killing (Fig 4H), indicating that in EGFR-TKI refractory tumors, secretion of IL-6 impairs NK cytotoxicity, and IL-6 blockade may at least partially restore NK cytotoxic potential.

IL-6 inhibits T cell activity in EGFR mutant NSCLC tumors

T cells are prominent effector cells in anti-tumor responses, and IL-6 has been shown to impair T cell anti-tumor activity [29, 30]. We evaluated T cells in tumors from murine $EGFR^{L858R}$ tumors with and without IL-6. We observed an increase in activated CD8+IFNγ+ T cell population in $EGFR^{L858R}/IL6^{tKO}$ tumors as compared to $EGFR^{L858R}$ tumors (Fig 5A; p=0.038). Similarly, $EGFR^{L858R}$ tumor-bearing animals treated with IL-6

antibodies also displayed a slight increase in the activated CD8+IFNγ+ T cell population compared to control mice (Fig 5B, Supplemental Fig 5A; p = 0.060). IL-6 has been shown to promote development of immunosuppressive Th17 T cell subsets [31]. We observed that the Th17 T cell subpopulation was reduced in $EGFR^{L858R}/IL6^{tKO}$ tumors as compared to $EGFR^{L858}$ tumors (Fig 5C; p = 0.048), and likewise Th17 T cells were reduced in $EGFR^{L858R}$ tumors treated with IL-6 blocking antibodies (p=0.032) (Fig 5D, Supplemental Fig 5B). Next, we incubated T cells derived from healthy donor PBMCs (Supplemental Fig 5C) with conditioned media from EGFR mutant HCC4006 cells, or their OR variants, with or without the IL-6 blocking antibody siltuximab. For T cells incubated with conditioned media from HCC4006 OR4 and OR7 cells, IL-6 blockade enhanced expression of granzyme B, an indicator of T cell activation and killing potential, (Fig 5E) but not perforin or Ki-67, which stimulate membrane disruption prior to cytotoxic killing and proliferation, respectively (Supplemental Fig 5D–E).

To assess the impact of IL-6 on T cell-mediated cytotoxicity, we co-cultured T cells with EGFR mutant tumor cells lines transfected to express membrane-bound anti-CD3 (OKT3), which binds CD3 on T cells and facilitates T cell killing independent of antigen-specific recognition. In EGFR-TKI refractory cells, IL-6 blockade significantly increased T cell-mediated killing (Fig 5F); IL-6 blockade did not, however, increase T cell mediated killing against HCC4006 parental cells which secrete markedly lower levels of IL-6.

Next, given that ICB therapy is driven by a T cell-mediated anti-tumor response, we assessed whether IL-6 blockade could enhance the activity of ICB against EGFR- mutant tumors. Consistent with clinical observations, single agent anti-PD-1 did not significantly improve overall survival in $EGFR^{L858R}$ syngeneic tumor-bearing mice (HR = 1.53, p= 0.310). Anti-IL-6 monotherapy, on the other hand, significantly extended overall survival in $EGFR^{L858R}$ tumor-bearing mice (HR= 2.30, p = 0.039). Combination treatment with anti-IL-6 with anti-PD-1 treatment even further increased overall survival (Fig 5G; HR = 3.15, p=0.016). Moreover, we observed an increase in the number of activated T cells (CD8+ PD-1+) in $EGFR^{L858R}$ tumors treated with the combination of anti-IL-6 and anti-PD-1 (Fig 5H; p=0.047), suggesting that IL-6 blockade may improve the efficacy of anti-PD-1 treatment, even in TKI-naïve models, in part by enhancing CD8 activation and IFNγ production (Fig 5A,B,&H).

Discussion

The cytokine IL-6 is known to associated with TKI resistance and have multiple potentially immunomodulatory effects. Given these observations, we hypothesized that IL-6 plays a role in the immunosuppressive, ICB-resistant immune microenvironment of EGFR mutant NSCLC. Furthermore, we hypothesized that this effect would be more pronounced in the setting of EGFR-TKI resistance, which is the relevant clinical setting in which these patients typically receive ICB.

To test this hypothesis, we characterized the immune landscape of murine models of treatment naïve and oncogene-independent EGFR-TKI resistance. In TKI-naïve EGFR mutant tumors, the presence of IL-6 was associated with reduced immune infiltration, which

could partially be reversed by IL-6 blockade. Depletion of IL-6 increased the infiltration and activation of both T and NK cells. This in vivo observation was supported by the in vitro finding that the tumor cell killing capacity of T and NK cells could be enhanced by IL-6 blockade. Finally, we demonstrate that in EGFR mutant tumor models, blockade of IL-6 enhances the efficacy of anti-PD-1 therapy.

The management of EGFR TKI refractory NSCLC is a major clinical challenge, and unfortunately, immunotherapy approaches have been unsuccessful in treating patients in the first line setting (ORR 9%) [5] and appear to be even less effective in the TKI refractory setting (ORR 5%). In an earlier retrospective cohort, monotherapy treatment with anti-PD-1/PD-L1 inhibitors managed a response rate of only 3.6% in EGFR mutant or ALK-positive patients compared to 23.3% in EGFR-wildtype and ALK-negative/unknown patients [12]. A meta-analysis showed that single agent ICB immunotherapy yielded worse results for patients with EGFR mutant lung cancers compared with docetaxel [8], and in retrospective analyses PD-1/PD-L1 inhibitors demonstrated a median progression-free survival (PFS) of 1.8 to 2.1 months [10, 11]. Attempts have been made to combine ICB immunotherapy with EGFR-TKIs; however, the prevalence of severe side effects prohibited the further development of these immune and targeted therapy combination approaches [32]. Studies are needed to identify factors that promote ICB immunotherapy resistance in the context of EGFR mutant NSCLC and identify biologically based combinatorial ICB immunotherapy strategies for these patients. In the present report, we investigated the role of IL-6 in driving ICB resistance in EGFR mutant NSCLC.

IL-6 is an inflammatory cytokine that has been associated with resistance to first, second, and third generation EGFR-TKIs through investigations by our group and others [14, 15]. Our previous study illustrated that IL-6 levels were not markedly elevated in EGFR mutant cells where EGFR-TKI resistance was associated with *MET* amplification or secondary EGFR mutations [14]. In the phase III ZEST clinical study, high plasma levels of IL-6 were associated with worse overall survival (OS) in unselected NSCLC patients treated with the EGFR-TKI erlotinib [14]. Additionally, a recent study also observed a positive association between high levels of circulating IL-6 with osimertinib, a third-generation EGFR-TKI, resistance[33]. While the increased IL-6 secretion observed in cells with acquired EGFR-TKI resistance has been shown to promote tumor cell survival and therapeutic resistance [14, 15, 33], the impact of elevated IL-6 in EGFR EMT-driven TKI resistant tumors on the tumor immune microenvironment has not been fully appreciated. Moreover, given the recent shift osimertinib to first-line treatment of EGFR mutant NSCLC patients, and the activity of osimertinib against the most common genomic mechanism of resistance to first- and second-generation TKIs (EGFR T790M secondary mutations) it is anticipated that EMT-mediated resistance will increase in frequency.

IL-6 has pleiotropic effects on effector cells in the anti-tumor response, promoting CD4+ T cell differentiation into T regulatory cells and inhibiting NK cell cytotoxicity. IL-6 has been implicated in promoting other immunosuppressive signalling pathways which may mediate resistance to ICB including the CD73-adenosine axis [34, 35]. We previously reported that CD73 expression is upregulated in EGFR mutant tumors compared to EGFR wildtype tumors [13]. Therefore, it is feasible that in EGFR-TKI resistant tumors

IL-6 upregulation may also drive an immunosuppressive microenvironment through CD73 signalling. Likewise, in EGFR mutant murine models of lung cancer, combination treatment of durvalumab (anti-PD-L1) and oleclumab (anti-CD73) exhibited synergistic anti-tumor effects[36]. This treatment combination treatments is under investigation in NSCLC patients including: oleclumab with osimertinib in NCT03381274 and durvalumab with oleclumab in the COAST (NCT03822351) [37] and NEOCOAST (NCT03794544) [38] trials. Therefore, we sought to investigate the role of IL-6 in the immunosuppressive EGFR mutant microenvironment, which is highly refractory to ICB immunotherapy. Because responses to ICB response are heavily dependent on immune effector cells, we investigated the effects of IL-6 on T and NK cell function in EGFR mutant NSCLC.

In the present report we utilized an immune-competent model of EGFR mutant NSCLC in which expression of the mutant EGFR transgene could be extinguished to characterize oncogene-independent, EGFR-TKI resistance. We find that unlike models studying tumor regrowth after discontinuing osimertinib [39, 40], this model is resistant to osimertinib dosing causing regression in the oncogene-dependent models, with tumors demonstrating EMT and increased IL-6 levels consistent with clinical resistance.

We find that the elevated expression of IL-6 associated with TKI resistance reduces the cytotoxic potential of T and NK cells in the EGFR mutant NSCLC microenvironment. Moreover, IL-6 increased the pro-tumorigenic Th17 T cell population and reduced infiltration of cytotoxic CD8+ T cells. Additionally, IL-6 reduced expression of activation markers like Granzyme B and NKG2D on tumor-infiltrating NK cells and by in vitro assays, IL-6 reduced the sensitivity of EGFR mutant TKI resistant cells to NK-mediated cytotoxicity. Consistent with our findings, studies in other malignancies have observed a similar role of IL-6 on impairing the function of infiltrating NK cells in the tumor microenvironment [28]. Additionally, other work has highlighted that mesenchymal tumors maybe more sensitive to NK-mediated cytotoxic killing than epithelial tumors [41]. These findings support our preclinical observation that NK-mediated cytotoxic killing occurs in the setting of EGFR-TKI resistant tumors treated with IL-6 blockade.

Previous studies in lung adenocarcinoma have highlighted a strong association between the mesenchymal status of tumors and a highly inflammatory tumor microenvironment. [27]. Currently, there are limited clinical approaches to overcome EMT-driven oncogene-independent TKI resistance. Here, by utilizing both cell line and GEM models, we observed that *IL6* expression is enhanced in EGFR mutant tumor cells which acquired EMT-associated EGFR-TKI resistance. These data indicate that IL-6 may be an actionable target to mitigate its role in promoting EMT-driven immunosuppression.

Using an EGFR mutant model of NSCLC, we show that blockade of IL-6 is more effective when used in combination with anti-PD-1 treatment, which resulted in an increase in overall survival. Together, these studies show that blockade of IL-6 favorably modulates the tumor immune microenvironment and enhances response to ICB predominantly through activation of T and NK cells. Futures studies should investigate the effect of IL-6 on macrophage infiltration given that myeloid cell immunosuppressive function and its subsequent effect on T reg and CD8 T cell.

Our previous studies identified a novel targetable mechanism of EGFR-TKI resistance by which stress hormones activate β2-adrenergic receptors and acutely upregulates IL-6. The present report elucidates an alternative mechanism of IL-6 upregulation which is EMT-associated. Therefore, both stress hormone signaling and EMT may be independent drivers of IL-6 mediated immunosuppression, and blockade of beta-adrenergic receptors may also suppress an IL-6-mediated immunosuppressive tumor microenvironment. Moreover, others have reported that metformin can block IL-6 expression and EMT in EGFR-TKI resistant cells [42]. Given that beta blockers and metformin are inexpensive and well-tolerated, the testing of these agents in combination with EGFR-TKIs and ICB should be considered. Agents targeting IL-6 are clinically available as FDA approved therapies. While in previous studies blocking IL-6 did not reverse TKI resistance when tested on EGFR mutant cells *in vitro* or *in vivo* using immunocompromised mouse models, the results reported here indicate that IL-6 blockade may, in part, reduce immunosuppression in the tumor environment. These findings support further investigation of IL-6 targeting in EGFR TKI refractory NSCLC as a therapeutic approach which may sensitize tumors to ICB therapy.

Supplementary Material

Refer to Web version on PubMed Central for supplementary material.

Acknowledgements:

This research was supported by the Emerson Collective, Lung SPORE grant 5 P50 CA070907, 1R01 CA190628, 1R01 CA234183-01A1, Stading Fund for EGFR inhibitor resistance, SP was supported by the CPRIT Training Award (RP210028), the Dr. John J. Kopchick Award, and the Schissler Foundation Award. The authors would like to thank the MD Anderson Flow Cytometry Core for supporting this project. The authors would like to also thank Dr. Katerina Politi for providing the YUL-0019 and $EGFR^{L858R}$ mouse model utilized in this paper.

Disclosures:

XL receives consulting/advisory fees from EMD Serono (Merck KGaA), AstraZeneca, Spectrum Pharmaceutics, Novartis, Eli Lilly, Boehringer Ingelheim, Hengrui Therapeutics, Janssen, Blueprint Medicines, Sensei Biotherapeutics, and Abbvie, and Research Funding from Eli Lilly, EMD Serono, Regeneron, and Boehringer Ingelheim. TC receives speaker fees/honoraria from The Society for Immunotherapy of Cancer, Bristol Myers Squibb, Roche, Medscape, and PeerView; advisory role/consulting fees from MedImmune/AstraZeneca, Bristol Myers Squibb, EMD Serono, Merck & Co., Genentech, and Arrowhead Pharmaceuticals; and institutional research funding from MedImmune/AstraZeneca, Bristol Myers Squibb, and EMD Serono. MBN receives royalties and licensing fees from Spectrum Pharmaceuticals. JVH serves on advisory committees for AstraZeneca, EMD Serono, Boehringer-Ingelheim, Catalyst, Genentech, GlaxoSmithKline, Guardant Health, Foundation medicine, Hengrui Therapeutics, Eli Lilly, Novartis, Spectrum, Sanofi, Takeda, Mirati Therapeutics, BMS, BrightPath Biotherapeutics, Janssen Global Services, Nexus Health Systems, Pneuma Respiratory, Kairos Venture Investments, Roche, Leads Biolabs, RefleXion, Chugai Pharmaceuticals, receives research support from Takeda, AstraZeneca, Boehringer-Ingelheim, and Spectrum, and receives royalties and licensing fees from Spectrum Pharmaceuticals. MBN receives royalties and licensing fees from Spectrum Pharmaceuticals. Y.Y.E. discloses research support from Spectrum, AstraZeneca, Takeda, Eli Lilly, Xcovery, and Tuning Point Therapeutics; and advisory role for AstraZeneca, Eli Lilly, and Turning Point; and accommodation expenses from Eli Lilly. S.J.M reports funding from Arrowhead Pharma, and Boehringer Ingelheim outside the submitted work. D.L.G reports advisory board work for AstraZeneca, Eli Lilly, Menarini Richerche, 4D Pharma, Onconova and Sanofi. D.L.G. receives research grant funding from AstraZeneca, Janssen, Astellas, Ribon Therapeutics, NGM Biotherapeutics, Boehringer Ingelheim and Takeda. M.C. reports grants and personal fees from ImmunoGenesis, Inc., personal fees from Alligator Bioscience, Inc., personal fees from ImmunOS, Inc., grants and personal fees from ImmunoMet, Inc., personal fees from Oncoresponse, Inc., personal fees from Pieris, Inc., personal fees from Nurix, Inc., personal fees from Aptevo, Inc., personal fees from Servier, Inc., personal fees from Kineta, Inc., personal fees from Salarius, Inc., personal fees from Xencor, Inc., personal fees from Agenus, Inc., personal fees from Mereo, Inc., personal fees from Amunix, Inc., personal fees from Adagene, Inc., outside the submitted work. M.C. has a patent Methods and Composition for Localized Secretion of Anti-CTLA-4 Antibodies with royalties paid to multiple licensees, a patent Dual specificity antibodies which bind both PD-L1 and PD-L2 and prevent their binding to PD-1 with royalties paid

to ImmunoGenesis, Inc., and a patent Cyclic Dinucleotides as Agonists of Stimulator of Interferon Gene Dependent Signaling licensed to ImmunoGenesis, Inc.

References

1. Midha A, Dearden S, and McCormack R, EGFR mutation incidence in non-small-cell lung cancer of adenocarcinoma histology: a systematic review and global map by ethnicity (mutMapII). Am J Cancer Res, 2015. 5(9): p. 2892–911. [PubMed: 26609494]
2. Gao J, et al. , Strategies to overcome acquired resistance to EGFR TKI in the treatment of non-small cell lung cancer. Clin Transl Oncol, 2019. 21(10): p. 1287–1301. [PubMed: 30864018]
3. Nilsson MB, et al. , A YAP/FOXM1 axis mediates EMT-associated EGFR inhibitor resistance and increased expression of spindle assembly checkpoint components. Sci Transl Med, 2020. 12(559).
4. Reita D, et al. , Molecular Mechanism of EGFR-TKI Resistance in EGFR-Mutated Non-Small Cell Lung Cancer: Application to Biological Diagnostic and Monitoring. Cancers (Basel), 2021. 13(19).
5. Lisberg A, et al. , A Phase II Study of Pembrolizumab in EGFR-Mutant, PD-L1+, Tyrosine Kinase Inhibitor Naive Patients With Advanced NSCLC. J Thorac Oncol, 2018. 13(8): p. 1138–1145. [PubMed: 29874546]
6. Borghaei H, et al. , Nivolumab versus Docetaxel in Advanced Nonsquamous Non-Small-Cell Lung Cancer. N Engl J Med, 2015. 373(17): p. 1627–39. [PubMed: 26412456]
7. Herbst RS, et al. , Pembrolizumab versus docetaxel for previously treated, PD-L1-positive, advanced non-small-cell lung cancer (KEYNOTE-010): a randomised controlled trial. Lancet, 2016. 387(10027): p. 1540–1550. [PubMed: 26712084]
8. Lee CK, et al. , Checkpoint Inhibitors in Metastatic EGFR-Mutated Non-Small Cell Lung Cancer-A Meta-Analysis. J Thorac Oncol, 2017. 12(2): p. 403–407. [PubMed: 27765535]
9. Rittmeyer A, et al. , Atezolizumab versus docetaxel in patients with previously treated non-small-cell lung cancer (OAK): a phase 3, open-label, multicentre randomised controlled trial. Lancet, 2017. 389(10066): p. 255–265. [PubMed: 27979383]
10. Negrao MV, et al. , Oncogene-specific differences in tumor mutational burden, PD-L1 expression, and outcomes from immunotherapy in non-small cell lung cancer. J Immunother Cancer, 2021. 9(8).
11. Mazieres J, et al. , Immune checkpoint inhibitors for patients with advanced lung cancer and oncogenic driver alterations: results from the IMMUNOTARGET registry. Ann Oncol, 2019. 30(8): p. 1321–1328. [PubMed: 31125062]
12. Gainor JF, et al. , EGFR Mutations and ALK Rearrangements Are Associated with Low Response Rates to PD-1 Pathway Blockade in Non-Small Cell Lung Cancer: A Retrospective Analysis. Clin Cancer Res, 2016. 22(18): p. 4585–93. [PubMed: 27225694]
13. Le X, et al. , Characterization of the Immune Landscape of EGFR-Mutant NSCLC Identifies CD73/Adenosine Pathway as a Potential Therapeutic Target. J Thorac Oncol, 2021. 16(4): p. 583–600. [PubMed: 33388477]
14. Nilsson MB, et al. , Stress hormones promote EGFR inhibitor resistance in NSCLC: Implications for combinations with beta-blockers. Sci Transl Med, 2017. 9(415).
15. Yao Z, et al. , TGF-beta IL-6 axis mediates selective and adaptive mechanisms of resistance to molecular targeted therapy in lung cancer. Proc Natl Acad Sci U S A, 2010. 107(35): p. 15535–40. [PubMed: 20713723]
16. Xu L, et al. , Epidermal growth factor receptor regulates MET levels and invasiveness through hypoxia-inducible factor-1alpha in non-small cell lung cancer cells. Oncogene, 2010. 29(18): p. 2616–27. [PubMed: 20154724]
17. Robichaux JP, et al. , Mechanisms and clinical activity of an EGFR and HER2 exon 20-selective kinase inhibitor in non-small cell lung cancer. Nat Med, 2018. 24(5): p. 638–646. [PubMed: 29686424]
18. Byers LA, et al. , Reciprocal regulation of c-Src and STAT3 in non-small cell lung cancer. Clin Cancer Res, 2009. 15(22): p. 6852–61. [PubMed: 19861436]

19. Nanjundan M, et al. , Proteomic profiling identifies pathways dysregulated in non-small cell lung cancer and an inverse association of AMPK and adhesion pathways with recurrence. J Thorac Oncol, 2010. 5(12): p. 1894–904. [PubMed: 21124077]
20. Arbiser JL, et al. , Oncogenic H-ras stimulates tumor angiogenesis by two distinct pathways. Proc Natl Acad Sci U S A, 1997. 94(3): p. 861–6. [PubMed: 9023347]
21. Politi K, et al. , Lung adenocarcinomas induced in mice by mutant EGF receptors found in human lung cancers respond to a tyrosine kinase inhibitor or to down-regulation of the receptors. Genes Dev, 2006. 20(11): p. 1496–510. [PubMed: 16705038]
22. Li T, et al. , TIMER2.0 for analysis of tumor-infiltrating immune cells. Nucleic Acids Res, 2020. 48(W1): p. W509–W514. [PubMed: 32442275]
23. Elamin YY, et al. , Poziotinib for EGFR exon 20-mutant NSCLC: Clinical efficacy, resistance mechanisms, and impact of insertion location on drug sensitivity. Cancer Cell, 2022. 40(7): p. 754–767 e6. [PubMed: 35820397]
24. Kapoor A, et al. , Yap1 activation enables bypass of oncogenic Kras addiction in pancreatic cancer. Cell, 2014. 158(1): p. 185–197. [PubMed: 24954535]
25. Ying H, et al. , Oncogenic Kras maintains pancreatic tumors through regulation of anabolic glucose metabolism. Cell, 2012. 149(3): p. 656–70. [PubMed: 22541435]
26. La Monica S, et al. , Third generation EGFR inhibitor osimertinib combined with pemetrexed or cisplatin exerts long-lasting anti-tumor effect in EGFR-mutated pre-clinical models of NSCLC. J Exp Clin Cancer Res, 2019. 38(1): p. 222.
27. Lou Y, et al. , Epithelial-Mesenchymal Transition Is Associated with a Distinct Tumor Microenvironment Including Elevation of Inflammatory Signals and Multiple Immune Checkpoints in Lung Adenocarcinoma. Clin Cancer Res, 2016. 22(14): p. 3630–42. [PubMed: 26851185]
28. Wu J, et al. , IL-6 and IL-8 secreted by tumour cells impair the function of NK cells via the STAT3 pathway in oesophageal squamous cell carcinoma. J Exp Clin Cancer Res, 2019. 38(1): p. 321.
29. Fisher DT, Appenheimer MM, and Evans SS, The two faces of IL-6 in the tumor microenvironment. Semin Immunol, 2014. 26(1): p. 38–47. [PubMed: 24602448]
30. Tsukamoto H, et al. , Combined Blockade of IL6 and PD-1/PD-L1 Signaling Abrogates Mutual Regulation of Their Immunosuppressive Effects in the Tumor Microenvironment. Cancer Res, 2018. 78(17): p. 5011–5022. [PubMed: 29967259]
31. Peng DH, et al. , Th17 cells contribute to combination MEK inhibitor and anti-PD-L1 therapy resistance in KRAS/p53 mutant lung cancers. Nat Commun, 2021. 12(1): p. 2606. [PubMed: 33972557]
32. Ahn MJ, et al. , 136O: Osimertinib combined with durvalumab in EGFR-mutant non-small cell lung cancer: Results from the TATTON phase Ib trial. J Thorac Oncol, 2016. 11(4 Suppl): p. S115.
33. Li L, et al. , Ibrutinib reverses IL-6-induced osimertinib resistance through inhibition of Laminin alpha5/FAK signaling. Commun Biol, 2022. 5(1): p. 155. [PubMed: 35197546]
34. Hu G, et al. , An IL6-Adenosine Positive Feedback Loop between CD73(+) gammadeltaTregs and CAFs Promotes Tumor Progression in Human Breast Cancer. Cancer Immunol Res, 2020. 8(10): p. 1273–1286. [PubMed: 32847938]
35. Zeng J, et al. , Mesenchymal stem/stromal cells-derived IL-6 promotes nasopharyngeal carcinoma growth and resistance to cisplatin via upregulating CD73 expression. J Cancer, 2020. 11(8): p. 2068–2079. [PubMed: 32127934]
36. Tu E, et al. , Anti-PD-L1 and anti-CD73 combination therapy promotes T cell response to EGFR-mutated NSCLC. JCI Insight, 2022. 7(3).
37. Herbst RS, et al. , COAST: An Open-Label, Phase II, Multidrug Platform Study of Durvalumab Alone or in Combination With Oleclumab or Monalizumab in Patients With Unresectable, Stage III Non-Small-Cell Lung Cancer. J Clin Oncol, 2022. 40(29): p. 3383–3393. [PubMed: 35452273]
38. Cascone T, Garcia-Campleo R, Spicer J, Weder W, Daniel D, Spigel D, Hussein M, Mazieres J, Oliveira J, Yau E, Spira A, Mager R, Hamid O, Cheng LY, Zheng Y, Blando J, McGrath L, Grenga I, Soo-Hoo Y, Kumar R, Forde P, Abstract CT011: NeoCOAST: open-label, randomized, phase 2, multidrug platform study of neoadjuvant durvalumab alone or combined with novel agents in

patients (pts) with resectable, early-stage non-small-cell lung cancer (NSCLC). Cancer Res, 2022. 82.

39. Higo H, et al. , EGFR-TKI acquired resistance in lung cancers harboring EGFR mutations in immunocompetent C57BL/6J mice. Lung Cancer, 2019. 136: p. 86–93. [PubMed: 31470227]
40. Mancini M, et al. , Generation and Characterization of a New Preclinical Mouse Model of EGFR-Driven Lung Cancer with MET-Induced Osimertinib Resistance. Cancers (Basel), 2021. 13(14).
41. Sheffer M, et al. , Genome-scale screens identify factors regulating tumor cell responses to natural killer cells. Nat Genet, 2021. 53(8): p. 1196–1206. [PubMed: 34253920]
42. Li L, et al. , Metformin sensitizes EGFR-TKI-resistant human lung cancer cells in vitro and in vivo through inhibition of IL-6 signaling and EMT reversal. Clin Cancer Res, 2014. 20(10): p. 2714–26. [PubMed: 24644001]

Translational relevance statement:

Alternate targeting of EGFR (epidermal growth factor receptor) mutant NSCLC (non-small cell lung cancer) tumors, a majority of which develop EGFR-TKI (tyrosine kinase inhibitor) resistance, is an unmet clinical need. Tumors which acquire resistance through EMT-associated EGFR-independent mechanisms are especially difficult to target. EGFR mutant NSCLC tumors are poorly responsive to immune checkpoint blockade (ICB) therapy further highlighting the need for new therapeutic approaches for TKI-resistant tumors. This study identified that EGFR mutant tumors which acquire oncogene-independent EGFR-TKI resistance express high levels of IL-6 and exhibit a more mesenchymal phenotype. Utilizing an immunocompetent murine model of EGFR mutant NSCLC, we show that IL-6 suppressed infiltration and cytotoxic potential of tumor-infiltrating NK and T cells. Blockade of IL-6 abrogated these immunosuppressive effects including a reduction in infiltrating T-regulatory and Th17 cell populations. Inhibition of IL-6 increased antitumor activity of ICB through increased infiltration of IFNγ+CD8+ T cells. These results support clinical testing of drugs targeting the IL-6 pathway in combination with ICB.

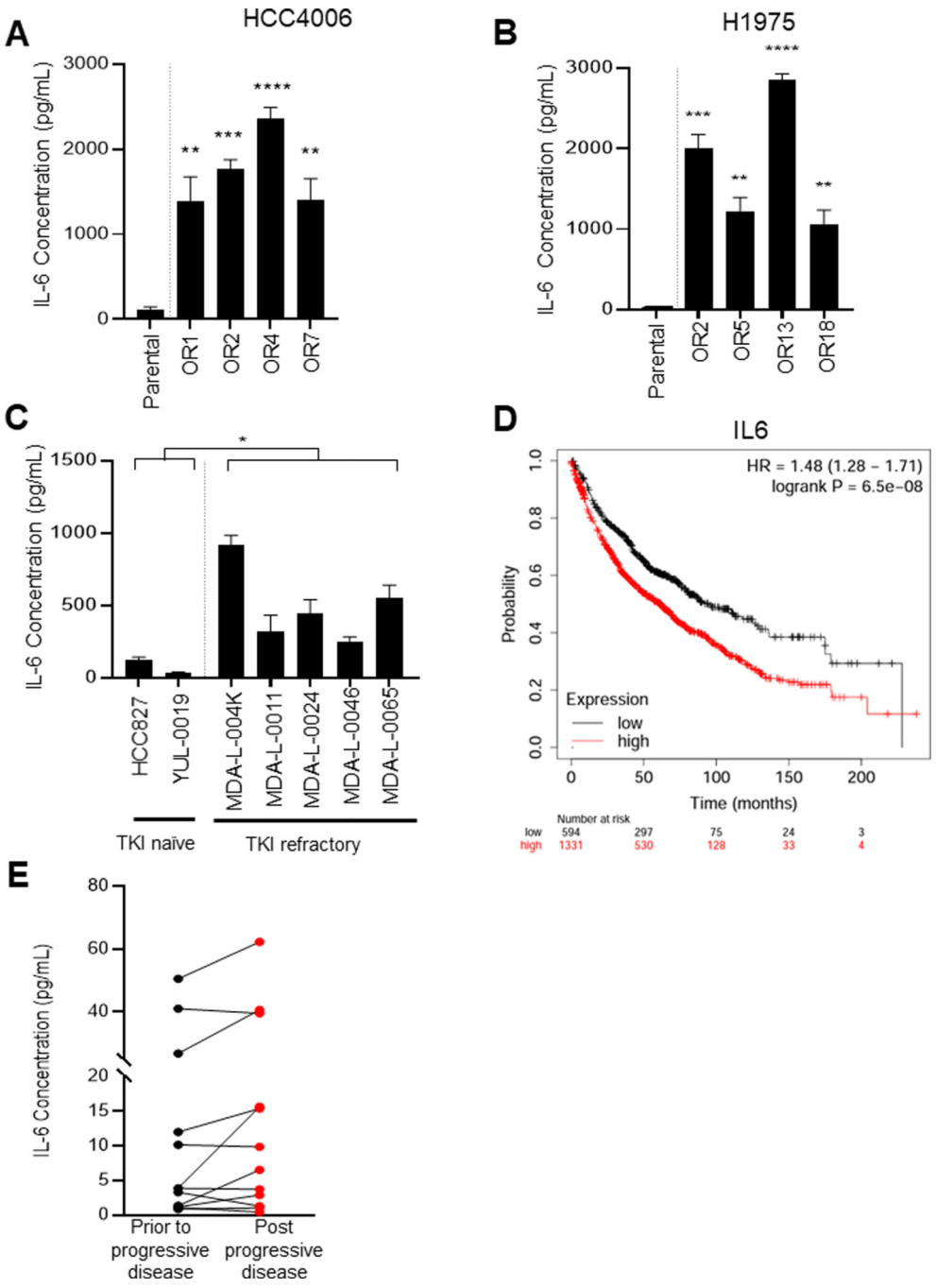

Figure 1 –.

EGFR mutant NSCLC tumor cells with acquired resistance to an EGFR-TKI have increased levels of IL-6. **(A&B)** ELISA analysis of IL-6 secretion by human EGFR mutant HCC4006 (A) and H1975 (B) cells and their osimertinib-resistant (OR) variants ($p < 0.0063$). **(C)** IL-6 production in EGFR mutant TKI naïve NSCLC cells (HCC827 and YUL-0019) and cell lines derived from EGFR mutant patients with acquired resistance to EGFR-TKIs ($p < 0.1509$). **(D)** Overall survival of EGFR mutation positive NSCLC patients from the KMplotter lung cancer dataset with high vs low *IL-6* expression ($n = 1926$, $p < 0.0001$). **(E)**

Circulating IL-6 levels were measured in patients from CROSSOVER and NORTHSTAR studies stratified by clinical outcome of prior to progression of disease or post progression of disease (n = 12 matched pairs run in duplicate, p =0.0517). (mean +/− SEM, * p<0.05, ** p<0.01, *** p<0.001)

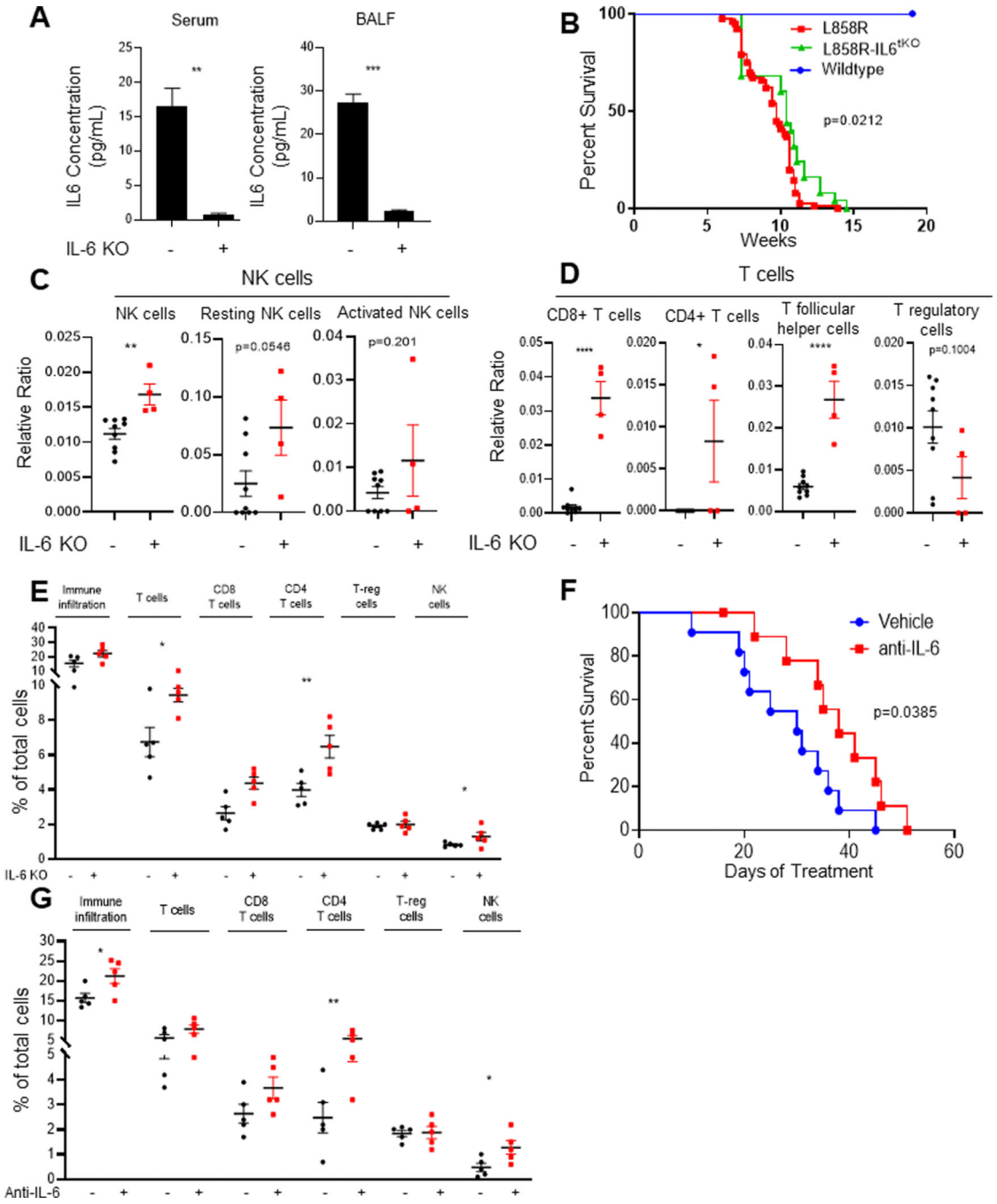

Figure 2 –.

Depletion of IL-6 increases the number of infiltrating lymphocytes and overall survival in EGFR mutant NSCLC tumors. **(A)** Expression of IL-6 in the serum and BALF of $EGFR^{L858R}$ and $EGFR^{L858R}$/ $IL6^{tKO}$ tumor-bearing mice. **(B)** Knockout of IL-6 extended the survival of $EGFR^{L858R}$ tumor-bearing mice (p = 0.0212). **(C-D)** Immune cell deconvolution analysis from RNA-sequencing data collected from control and IL-6 knockout tumors from $EGFR^{L858R}$ mice showed a minor decrease in T-regulatory cells (p = 0.1004) and a slight increase of CD8+ T cells (p = 0.0595), CD4+ T cells (p = 0.0086),

NK cells ($p = 0.0032$) and T follicular helper cells ($p < 0.0001$). **(E)** Tumor immune cell populations in $EGFR^{L858R}$ tumors with or without anti-IL-6 treatment as determined by flow cytometry. **(F)** Kaplan-meier analysis of EGFR mutant GEMM treated acutely with monoclonal blocking antibody to IL-6 ($p = 0.0385$). **(G)** Flow cytometry analysis to directly assess infiltrating immune cells in T and NK cell infiltration in EGFR mutant GEMM treated with monoclonal blocking antibody to IL-6. (mean +/− SEM, * $p<0.05$, ** $p<0.01$, *** $p<0.001$)

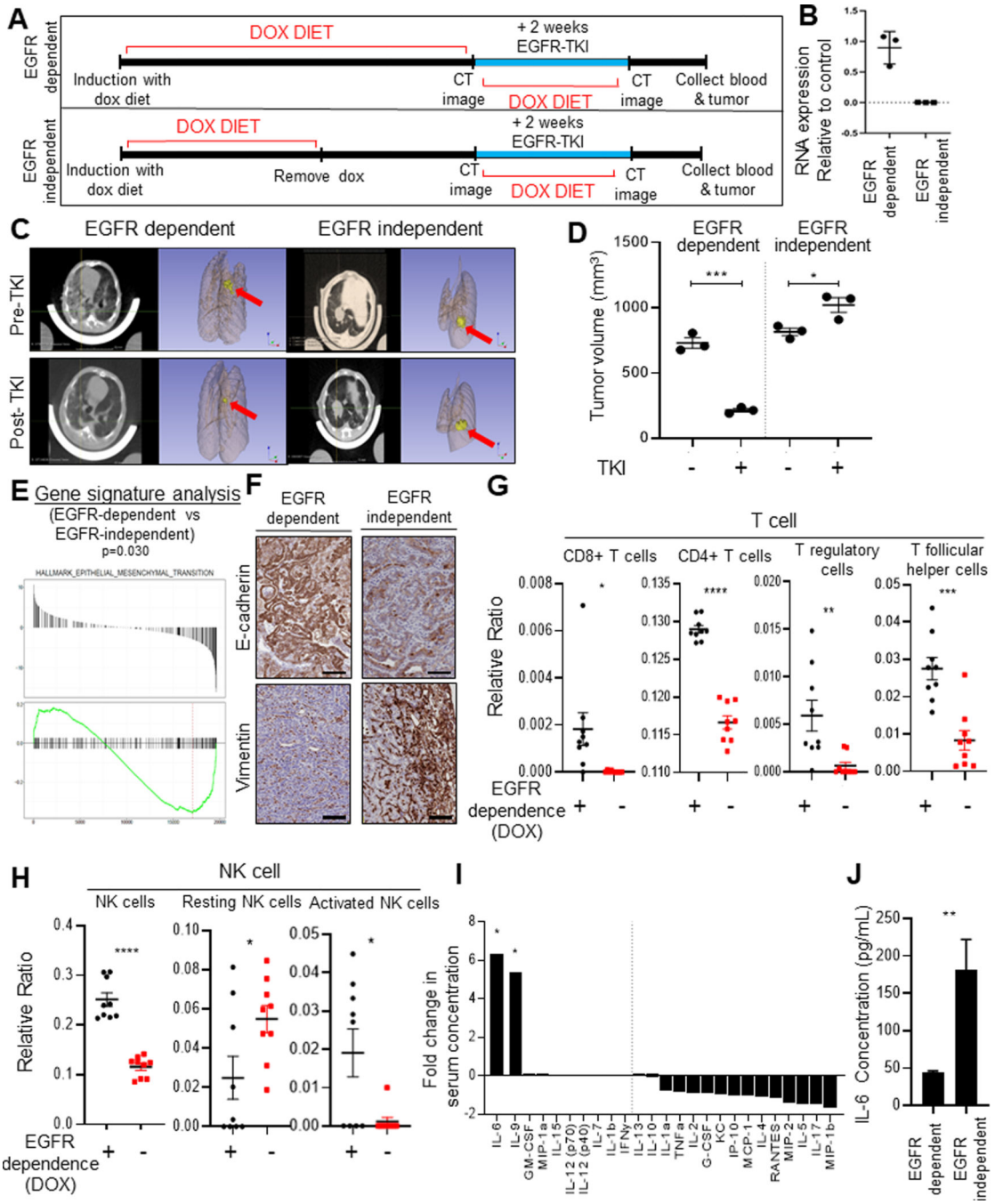

Figure 3 –.

Oncogene-independent EGFR-TKI resistant EGFR mutant NSCLC tumors display an immunologically cold, mesenchymal phenotype. **(A)** Timeline of induction or withdrawal of doxycycline used as an inducing agent for the generation of EGFR mutant lung tumors in GEMMs. **(B)** Levels of *EGFR* are measured by qPCR of RNA collected from tumors collected from the oncogene-dependent (dox on) and oncogene-independent (dox off) models displaying a significant decrease in *EGFR* expression in the dox off samples. **(C)** CT imaging and **(D)** associated quantification displaying the significant increase in tumor

volume ($p = 0.0475$) in the dox off tumor during EGFR-TKI treatment. **(E)** Oncogene-independent tumors display an enrichment of an epithelial-to-mesenchymal phenotype. **(F)** Oncogene-independent tumors show an increased expression of vimentin and loss of E-cadherin. **(G-H)** Immune cell deconvolution analysis from RNA-sequencing data collected from oncogene-dependent and oncogene-independent tumors showed a significant reduction of CD8+ T cells ($p = 0.0194$), CD4+ T cells ($p < 0.0001$), total NK cells ($p < 0.0001$), activated NK cells ($p = 0.0122$), and T follicular helper cells ($p = 0.0061$). **(I)** Multiplex ELISA analysis of serum collected from oncogene-dependent compared to oncogene-independent tumor-bearing mice. **(J)** IL-6 ELISA confirms elevated levels of IL-6 in oncogene-independent model compared to oncogene-dependent. (mean +/− SEM, * $p<0.05$, ** $p<0.01$, *** $p<0.001$)

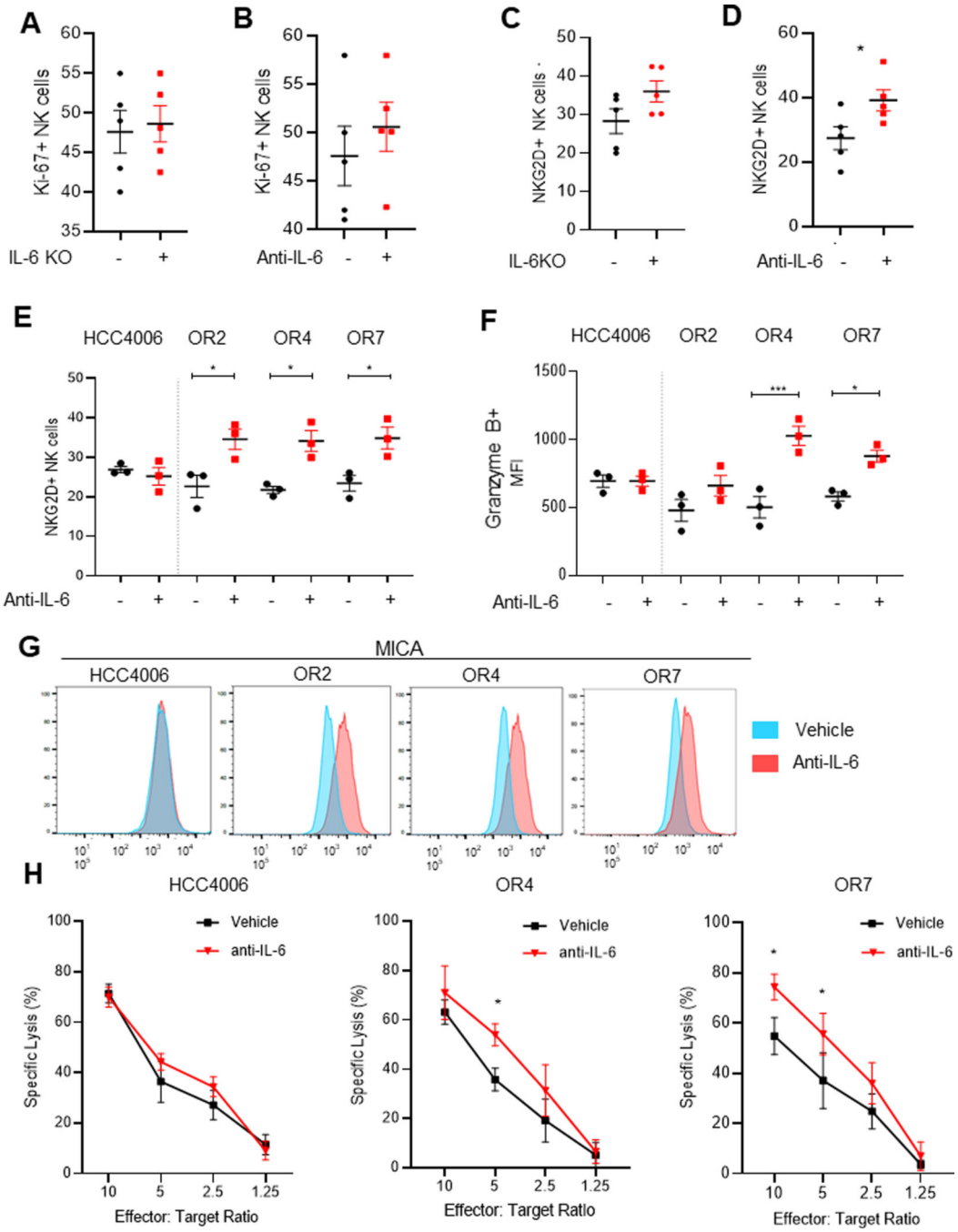

Figure 4 –.

IL-6 suppresses the activation of NK cells in EGFR mutant NSCLC tumors. **(A)** IL-6 knockout and **(B)** acute blockade of IL-6 increases expression of Ki-67+ proliferating NK cells (p=0.3501, p=0.4698), **(C-D)** activated NKG2D+ NK cells) (p=0.1042, p=0.0418). **(E-F)** Acute blockade of IL-6 of EGFR mutant NSCLC cell lines co-cultured with human NK cells isolated from healthy donor PBMCs significantly increased expression of NKG2D and Granzyme NK cells **(G)** MICA expression on EGFR mutant TKI resistant is increased

with IL-6 blockade. **(H)** IL-6 blockade sensitizes EGFR mutant EGFR-TKI resistant cells to NK cell-mediated cytotoxic killing. (mean +/− SEM, * $p<0.05$, ** $p<0.01$, *** $p<0.001$)

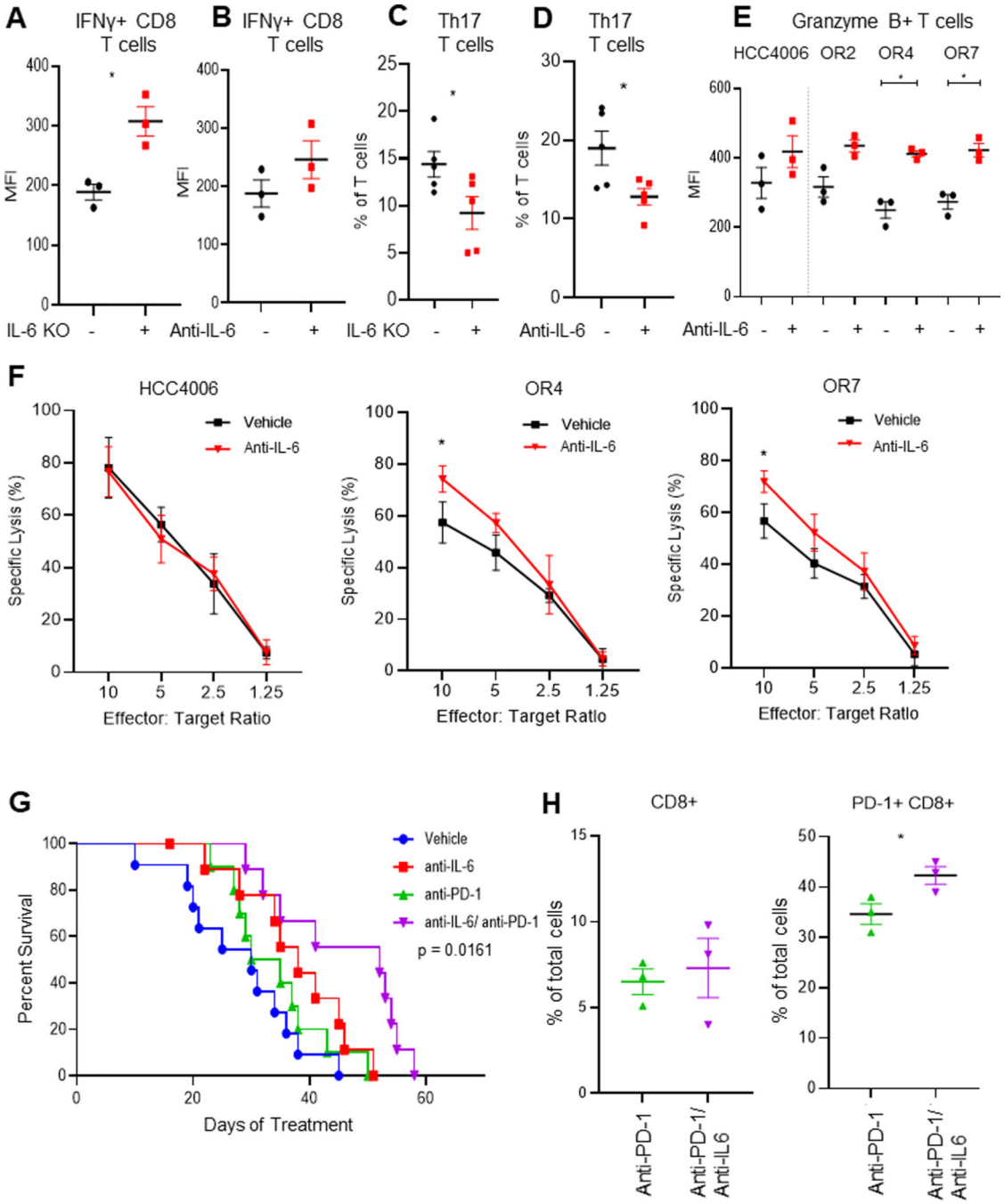

Figure 5 –.

IL-6 inhibits T cell-mediated anti-tumor response in EGFR mutant NSCLC tumors. **(A-D)** IL-6 knockout increased CD8+IFNγ+ T cells (p=0.0375) while IL-6 blockade had slightly more modest effects p=0.0375. Th17 T cell populations were significantly reduced in IL-6 knockout tumors (p=0.048) and those treated with IL-6 blocking antibody (p=0.032). **(E)** Human T cells isolated from healthy donor PBMCs co-cultured in conditioned media collected after the acute blockade of IL-6 of EGFR mutant NSCLC cell lines significantly increased expression of Granzyme B expression. **(F)** Anti-IL-6 treatment increased T cell-

mediated cytotoxicity of EGFR mutant NSCLC cell lines. **(G)** Anti-IL-6 blockade induces increased survival of EGFR mutant GEMMs treated with anti-PD-1 immunotherapy ($p = 0.0161$). **(H)** Anti-IL-6 and anti-PD-1 combination treatment increases infiltration of activated T cells (PD-1+ CD8+) in EGFR mutant GEMMs ($p = 0.0468$). (mean +/− SEM, * $p<0.05$, ** $p<0.01$, *** $p<0.001$)